Supplementary Material

O. Urban *et al.*: Tree-ring stable isotopes and growth trajectories reveal early warning signals of drought-induced Scots pine mortality

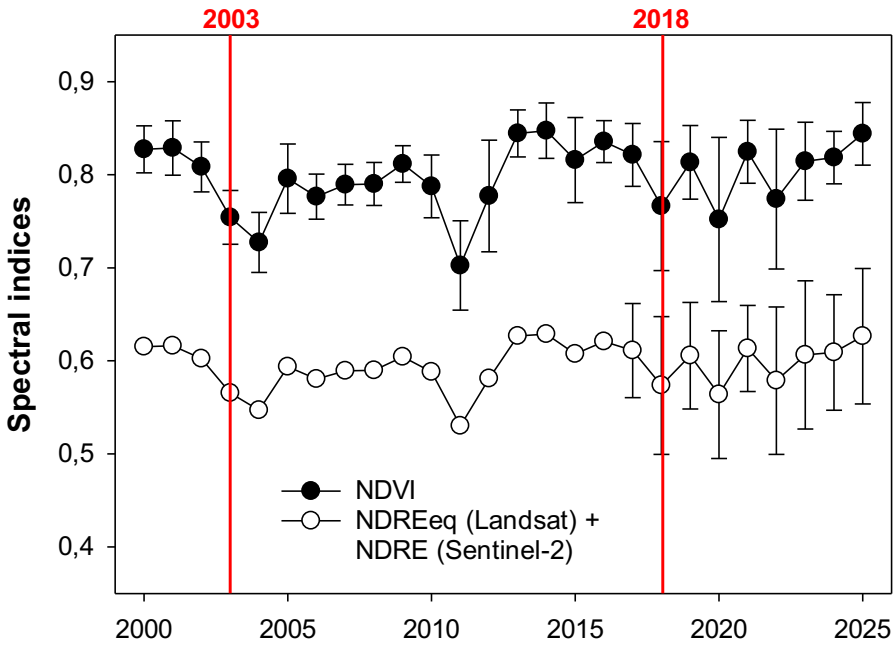

Figure S1. Interannual variability in canopy greenness and red-edge chlorophyll-proxy indices for a 2-ha region of interest (ROI) centred at 50°00'44.0"N, 8°11'23.7"E in the Lenneberg Forest (Mainz, western Germany). Filled circles indicate Landsat-derived NDVI (2000–2025), while open circles represent a combined series of red-edge NDRE values: Landsat-based NDREeq (NDRE-equivalent) estimates for 2000–2016 and Sentinel-2 NDRE measurements for 2017–2025. Each point reflects the mean of summer (June–August) per-pixel median composites across all valid cloud-free pixels within the ROI; error bars indicate ±1 SD (spatial heterogeneity). Vertical red lines mark the extreme drought years 2003 and 2018, which coincide with marked drops in NDVI and NDRE. NDVI = (NIR − red)/(NIR + red), derived from Landsat sensors using standard near-infrared and red bands. Sentinel-2 NDRE = (NIR − red-edge)/(NIR + red-edge), calculated from bands B8 (842 nm) and B5 (705 nm). Due to the absence of red-edge bands in Landsat, NDREeq values were calculated via linear regression between Sentinel-2 NDRE and overlapping Landsat NDVI observations from 2017–2025 (NDREeq = 0.0514 + 0.6814 × NDVI; R^2 = 0.61, n = 9). Data processing was performed in Google Earth Engine (GEE); see Methods for details.

Remote-sensing data retrieval and index calculation. Remote-sensing processing was performed in Google Earth Engine (GEE). The ROI was defined as a circular buffer with an area of 2 ha around the centre coordinates given above. Landsat data were obtained from Collection 2, Tier 1, Level 2 surface reflectance products for Landsat 5 TM (LANDSAT/LT05/C02/T1_L2), Landsat 7 ETM+ (LANDSAT/LE07/C02/T1_L2), Landsat 8 OLI (LANDSAT/LC08/C02/T1_L2) and Landsat 9 OLI-2 (LANDSAT/LC09/C02/T1_L2). Sentinel-2 data were obtained from the harmonized surface reflectance product (COPERNICUS/S2_SR_HARMONIZED). For each sensor and year, all scenes intersecting the ROI in June–August were collected. Clouds, cloud shadows, cirrus and snow/ice were masked using the QA_PIXEL bitmask for Landsat (cloud shadow, snow, cloud, cirrus) and the Scene Classification Layer for Sentinel-2 (SCL classes 3, 8–11). Landsat reflectance scaling followed the Collection 2 Level 2 definition (reflectance = DN × 0.0000275 − 0.2). Annual summer composites were calculated using the per-pixel median of all valid observations within the seasonal window. ROI-level means and standard deviations were computed from the composite images at the native spatial resolution (30 m for Landsat; 10 m for Sentinel-2). Years with no valid observations after masking were treated as missing. The combined NDRE series in this figure uses Landsat-derived NDREeq for 2000–2016 and Sentinel-2 NDRE for 2017–2025.

Figure S2. Monthly response of basal area increment (BAI) to environmental variables. Values of correlation coefficients between monthly environmental variables and BAI for the period 1930–2019. Colours denote vitality classes: dark green = all trees combined, light green = Class 1 (vigorous), yellow = Class 2 (intermediate), red = Class 3 (poor vigour). Transparent bars indicate non-significant correlations ($p \geq 0.05$). Climate variables include monthly temperature, precipitation, potential evapotranspiration (PET), and soil moisture index (SMI). See Methods for data sources and correlation procedures.

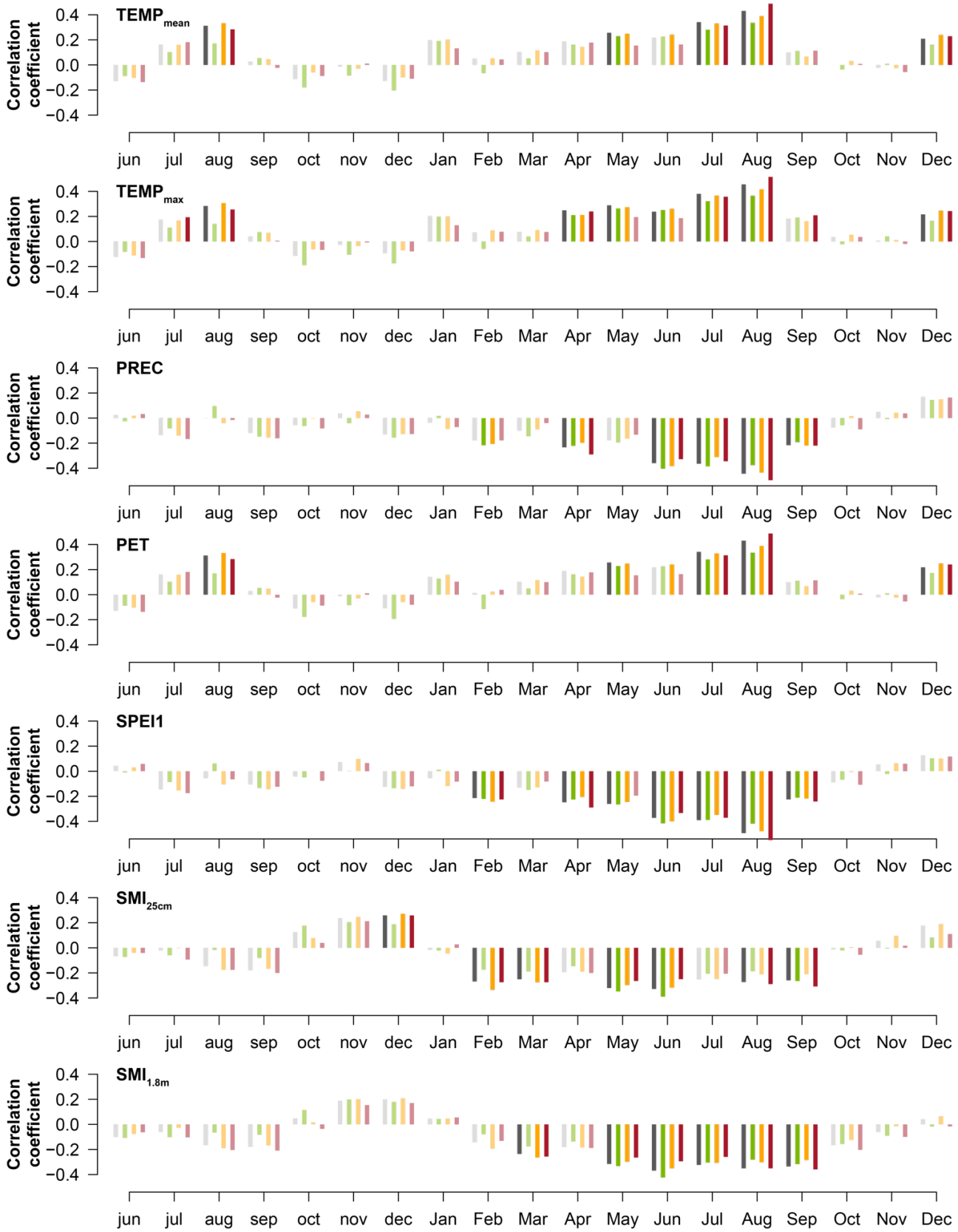

Figure S3. Monthly response of $\delta^{13}C$ to environmental variables. Correlation coefficients between monthly climate parameters and tree-ring $\delta^{13}C$ values over the period 1930–2019. Vitality classes are colour-coded as in Fig. S2. Statistically non-significant correlations are shown as transparent bars. $\delta^{13}C$ values were corrected for atmospheric changes (Suess effect); see Methods for analytical and statistical details.

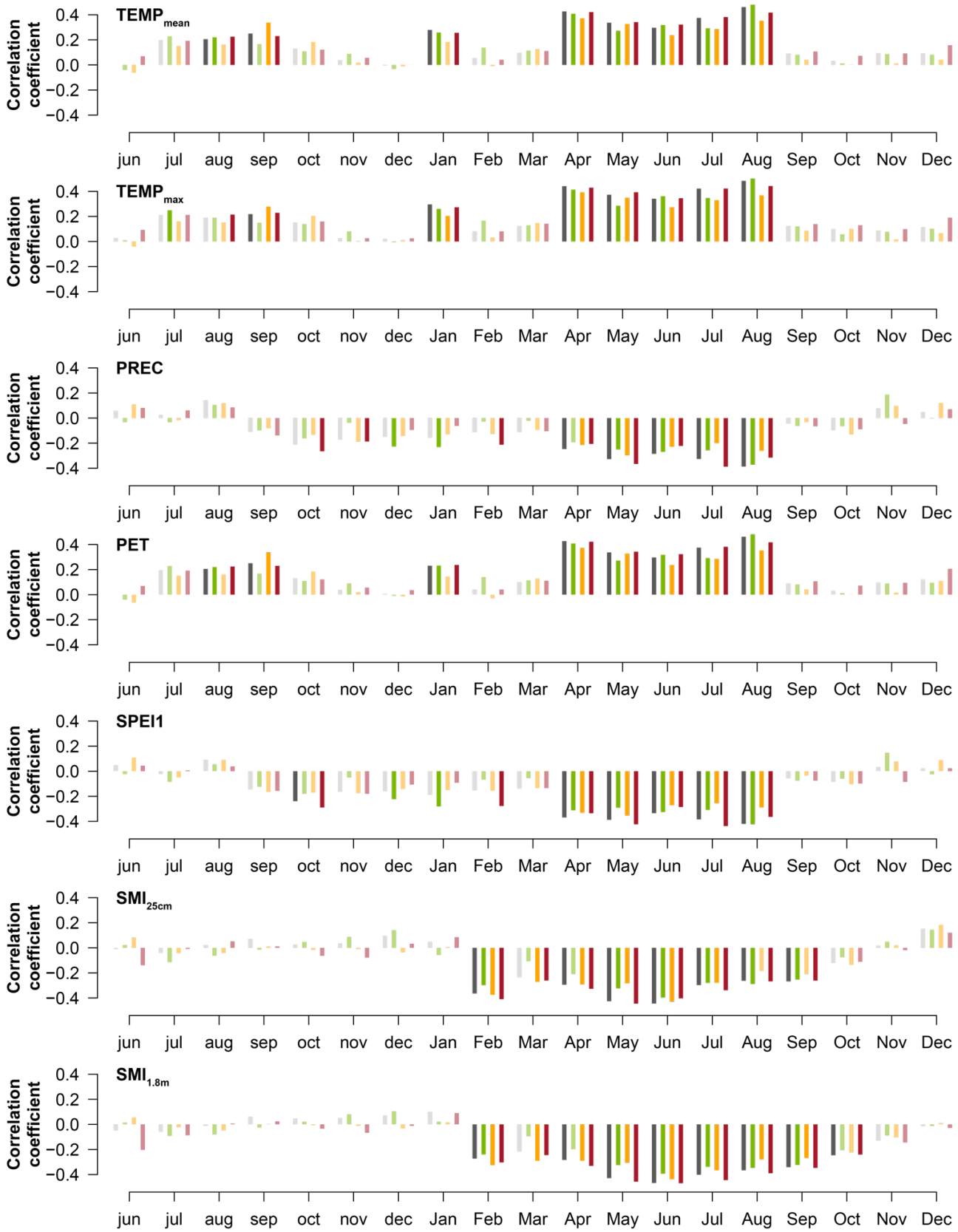

Figure S4. Monthly response of $\delta^{18}O$ to environmental variables. Values of correlation coefficients between monthly climate parameters and $\delta^{18}O$ values in tree-ring cellulose from 1930–2019. Colours and significance indications follow the conventions used in Figs. S2 and S3. See Methods for isotope analysis and climate data processing.

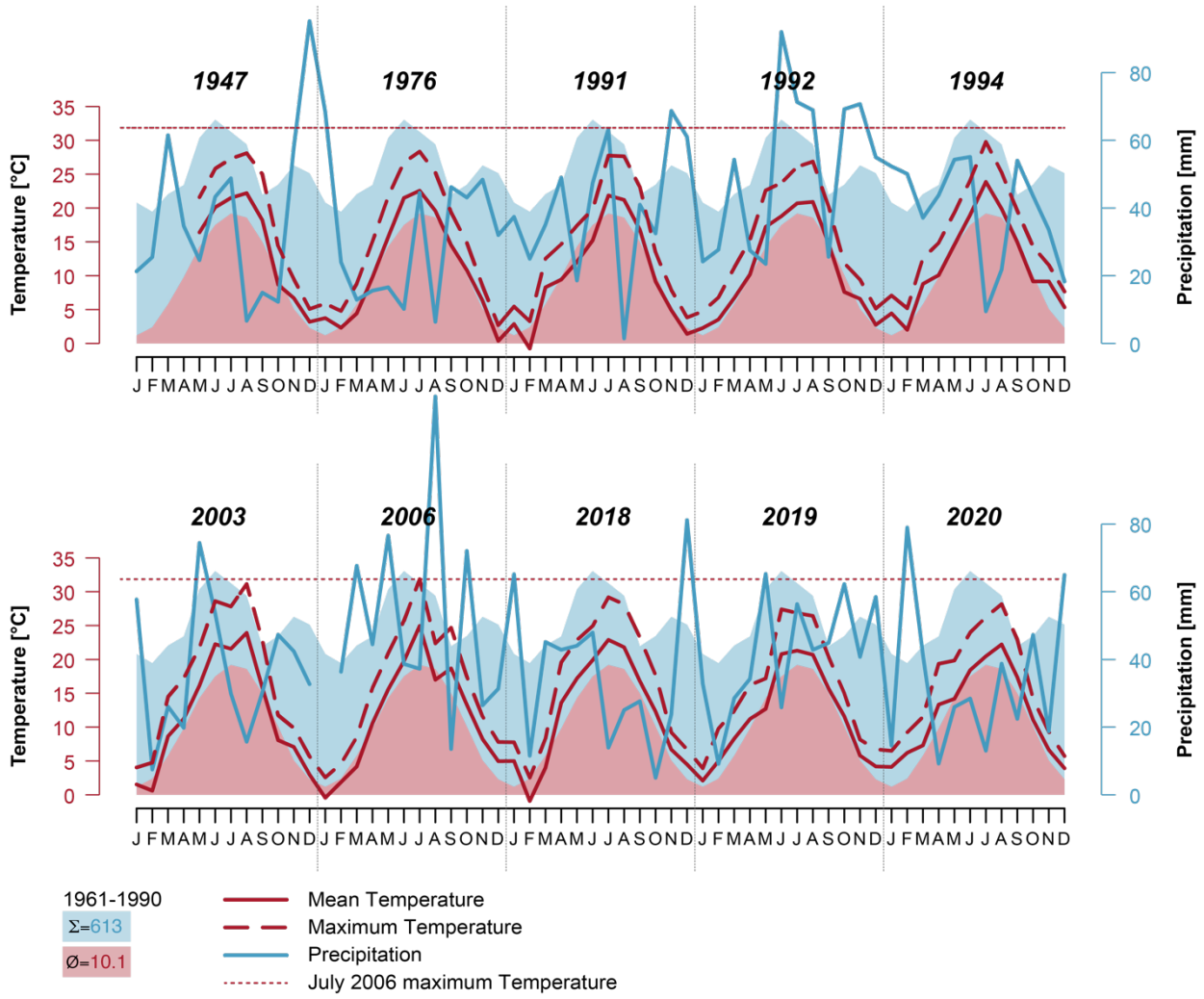

Figure S5. Climatic conditions during specific years (lines) with respect to the 1961–1990 reference period (area signatures) based on DWD climate data from Mainz.